Transmission Adaptive Capacity-Based Resilience Metrics for Power Grid Contingency Analysis

Jianzhong Gui, Hangtian Lei, Yacine Chakhchoukh, Timothy R. McJunkin, and Brian K. Johnson

***Abstract*—Power system resilience generally represents the capability of the system recovering from a degraded state to normal operation in an acceptable period of time. In power systems, status changes of transmission lines are typically caused by events such as varying load, changes in non-dispatchable generation, transmission line opening, or generating power shedding. The adaptive capacity of the transmission network represents its power transmitting ability to adjust to these status changes and still meet the load demand. In this paper, we propose resilience metrics based on transmission adaptive capacity to quantitatively represent system resilience in response to events. Case studies are designed and performed in the IEEE 14-bus and 118-bus test systems using the MATPOWER platform. Simulation results demonstrate the validity of the proposed resilience metrics.**

***Index Terms*—Contingency, generation shedding, load demand, resilience, transmission lines.**

I. Introduction

The resilience of power systems represents the system defending, resisting, and recovering processes under disturbances [1]-[3]. The characteristics of resilience are used in assessing schemes for monitoring, control, and protection of power systems to mitigate the consequences caused by major disturbances, system malfunctioning, cyber-physical attacks, and natural disasters [4]-[10].

Resilience metrics provide a quantitative representation of system recovery performance, and the results of different types of metrics can be utilized for applications ranging from planning, operation, to disaster mitigation processes. Reference [11] proposes resilience metrics for protection systems, and provides a level of state awareness with distributed resilience metrics which could be used in supervisory control and data acquisition (SCADA) or other communication schemes. The authors in [12] define regional resilience with necessary metrics to identify unreliable operating states, which is assessed by distributed agents with monitoring and analyzing functions.

Researchers have proposed resilience metrics that evaluate different characteristics for distribution systems in recent years [13]-[18]. Reference [14] defines the resilience metrics for distribution systems, and addresses the adaptive capacity of the power system in response to disturbances. An efficient algorithm to solve a nonconvex problem, which is formulated to reduce losses and improve system resilience, is proposed in [15] to optimize the operation of distribution grids. In [16] and [17], the resilience characteristics are evaluated for distribution service and formation of microgrids under natural disasters. In [18], the configuration and key benefits of having resilient distribution systems in smart grids are introduced, and the installation principles are compared between traditional and modern resilient distribution systems. Possible evaluation frameworks for the contribution of renewable energy resources to resilience are constructed in [19] and [20]. In [19], the resilience contribution of solar PV and battery storage are assessed with a quantifiable adaptive capacity measure. In [20], a response metric is provided to express the resilience contribution of hydropower generation, which includes the storage states features and plant level constraints on power production.

Based on the proposed quantitative resilience metrics, several methods have been discussed for system resilience improvement [21], [22]. The combination of reliability and resilience information is considered in [21] to improve the reliability and resilience at the same time during the process of load shedding. A modeling method to assess system resilience is proposed in [22], which is performed under the changing intensity of wind storms. Although the proposed model is only verified under the current climate, it provides a useful way to identify the potential risk of future climate hazards to electricity infrastructure networks.

It is necessary to pay attention to critical branches, especially when the changed flows impact the status of the branches. In a small power system, the status of these branches can be monitored directly, but it is difficult to monitor and display the remaining capacity of every branch for a large power system in a fashion the operator can take in. Therefore, we propose a resilience metric to display the overall status of the transmission network which provides concise information to facilitate operators' actions.

An operational resilience metric based on transmission adaptive capacity will be developed to quantitatively represent system resilience in response to events that have occurred on the system. The capacity margins of transmission lines are adjusted depending on the impact of disturbances and attacks. The remaining capacity represents the resilience of power transmitting capability. The proposed resilience metric is verified under several different adversary scenarios.

This paper is organized as follows. The concept of transmission line resilience is introduced in Section II. The resilience metric based on power transmitting capacity of branches is proposed and illustrated in Section III. Case studies based on the proposed resilience metrics are performed in Section IV. Finally, conclusions are drawn in Section V.

This work was supported through the INL Laboratory Directed Research and Development (LDRD) Program under DOE Idaho Operations Office Contract DE-AC07-05ID14517.

J. Gui, H. Lei, Y. Chakhchoukh, and B. K. Johnson are with the Department of Electrical and Computer Engineering, University of Idaho, Moscow, ID 83843, USA (e-mails: gui2361@vandals.uidaho.edu; hlei7@uidaho.edu; yacinec@uidaho.edu; bjohnson@uidaho.edu).

T. R. McJunkin is with Idaho National Laboratory, Idaho Falls, ID 83415, USA (e-mail: timothy.mcjunkin@inl.gov).

2021 North American Power Symposium (NAPS) | 978-1-6654-2081-5/21/$31.00 ©2021 IEEE | DOI: 10.1109/NAPS52732.2021.9654605

XXX-X-XXXX-XXXX-X/XX/$XX.00 ©20XX IEEE

Authorized licensed use limited to: b-on: Universidade de Coimbra. Downloaded on April 27,2025 at 06:58:05 UTC from IEEE Xplore. Restrictions apply.

II. The Resilience of Transmission Lines

The structure of transmission network and the adequacy of transmission capacity are vitally important to understanding the resiliency of power systems in response to contingency events in planning studies.

In the example shown in Fig. 1, each load is supported by two generators. If the generator at Bus 2 is disconnected due to attacks or other disturbances, the generators at Buses 1 and 3 will send more power through the branch from Bus 4 to Bus 5, and the branch from Bus 9 to Bus 8. As a result, the power flow on the two branches may exceed their set transmission limit based on thermal ratings or stability limits.

Similarly, if the circuit breakers on the branch from Bus 4 to Bus 6 are tripped due to a fault, the power supporting the load on Bus 6 has to be re-routed to the branch from Bus 9 to Bus 6, which will increase the power flow on that branch.

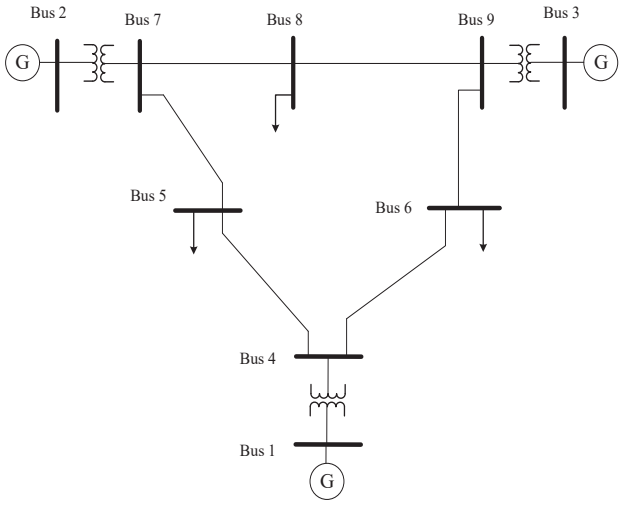

Fig. 1. Nine-bus example power system.

A transmission line connected between two substations has the ability to transmit power from one side to the other side. The thermal capacity for transmitting power depends on the line materials and types and meteorological conditions. The actual usage of power transmission capacity is represented by the transmission line loading rate (LR), as shown in (1).

The line loading rate can be calculated by the following equation:

$$LR = \frac{S_{Actual}}{S_{Capacity}} \times 100\% \quad (1)$$

Where S_{Actual} is the actual apparent power transmitted in the transmission line, $S_{Capacity}$ is the transmission capacity of the line.

The remaining power capacity (RPC) can be computed by subtracting the line loading rate from the line capacity, as shown in Fig. 2 and equation (2).

$$RPC = (1 - LR) \times S_{capacity} \quad (2)$$

Where $S_{Capacity}$ is the transmitting capacity of the transmission line.

The loading of transmission lines can be adjusted by changing the output power at generating buses. The resilience of a transmission line is the remaining power capacity (RPC) for transmitting power between substations. Taking loading status of all branches (including transformer branches) into consideration, the resilience of transmitting power plays a role in evaluating the operation state of power systems.

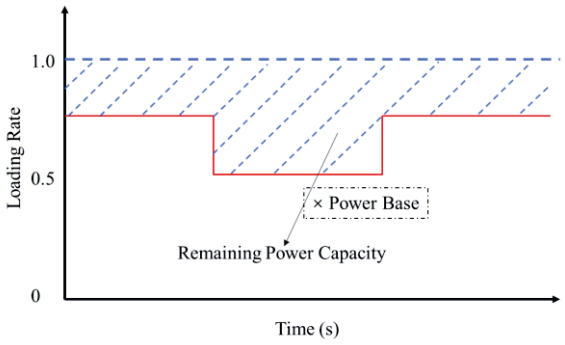

Fig. 2. The diagram of loading curve for a transmission line.

The number of transmission lines with overloaded status in a system can be counted, but it is inconvenient to display the status of all lines individually. For a limited number of transmission lines, the overload status can be displayed by showing the loading rate of each transmission line. However, displaying the status of a large number of transmission lines individually introduces difficulties to understand the status of the whole system. Therefore, the metric considering the operation states of all transmission lines is needed. With such metrics, it is convenient to know and compare the differences among various operation scenarios of the power system.

III. Resilience Metrics Based on Transmitting Capacity of Transmission System

In order to quantify the resilience of transmission lines, the metrics depending on the loading rate is proposed in detail in this section. The loading rate of a transmission line is calculated using the active power and reactive power flow in each branch. The number of overloaded branches is used for the calculation of the proposed resilience metric.

A. The Proposed Resilience Metric

The proposed resilience metric, marginal capacity percentage, is shown in (3).

$$r = 1 - p \quad (3)$$

Where r is the marginal capacity percentage and p is the percentage of transmission lines whose loading exceeds 90% of their capacities.

The percentage can be calculated as following:

$$p = \frac{n}{N} \times 100\% \quad (4)$$

Where n is the number of transmission lines whose loading are 90% or higher. N is the total number of transmission branches.

The line loading rate can be calculated using equation (1).

Authorized licensed use limited to: b-on: Universidade de Coimbra. Downloaded on April 27,2025 at 06:58:05 UTC from IEEE Xplore. Restrictions apply.

B. The Resilience Characteristics

For a transmission system, the resilience metric value changes when the system is disrupted by major generation change, major load change, transmission faults that result in lockout of the line, or cyber or physical attacks which may cause transmission lines open. During a period of system operation, the metric value varies due to the change of system operating conditions. A sketch of the resilience metric value (r) versus time curve is shown in Fig. 3.

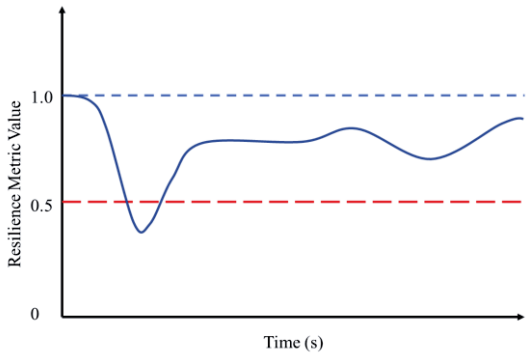

Fig. 3. A sketch of power system resilience metric curve under disturbances.

The maximum value of r is 1, and the minimum is 0. A bigger value of r indicates that the line status is better than a smaller one. According to utility practice, the system is allowed to operate for a period of time even when the power flows on some lines exceed the limits. A bigger r for the system indicates a longer period of time of allowed operation.

IV. Case Study

A. Simulation Description

The simulation is performed using MATPOWER. The power flow function based on MATLAB is programed with customized contingency analysis codes.

The IEEE 14-bus and IEEE 118-bus systems are used in the case studies in this section. A 1.25-time basic power flow in transmission line is set as the power base for each branch. The line loading rates in (1) are calculated using these bases. The basic power flow is calculated in the power flow routine in MATPOWER [23], [24]. For the contingency analysis, the output of generators, the load demand, and transmission line operation status are taken into consideration.

B. Case Simulation using the IEEE 14-Bus System

In the IEEE 14-bus system, Bus 1 is considered as the slack bus which is treated as representing a connection to a larger power grid. The remaining generators are controlled as PV buses. The real power (P) in the base case, maximum real power, and maximum reactive power for buses 2, 3, 6, and 8 are shown in Table I.

TABLE I. Base Case Power of PV Bus Generators with Limits

Bus No.	2	3	6	8
Actual P/MW	40	0	0	0
P_{MAX}/MW	140	100	100	100
Q_{MAX}/Mvar	50	40	24	24

There are 14 buses, 5 generators, 11 loads, and 20 branches (transmission line and transformer branches) in the IEEE 14-bus system [25], as shown in Fig. 4.

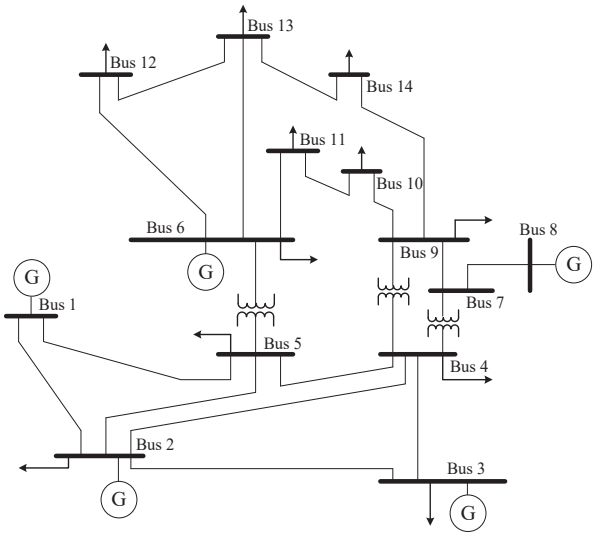

Fig. 4. The single-line diagram of IEEE 14-bus system.

The following contingency categories are investigated in the analysis, with metric values computed to approximate different operating cases that an operator would experience.

1) One Transmission Line Open

The simulation is performed by disconnecting one transmission branch at a time. There are 20 scenarios in this contingency category. The metric values using (3) are shown in Fig. 5.

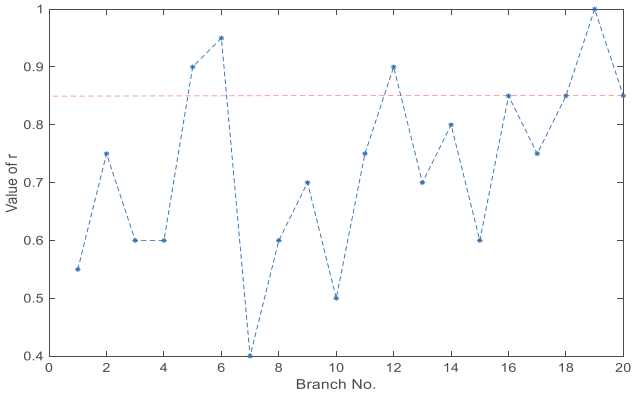

Fig. 5. The metric values under different open-line conditions.

From Fig. 5, it can be seen that opening Branch 7 could push multiple transmission lines to have capacity margins less than 10%, and are possibly into overload status. From the view of operation, ensuring the security of operation on Branch 7 could improve the resilience of the system. This means an operator would need to choose generator set points to ensure this condition would not compromise the resilience of the system.

Setting 0.85 as a threshold as indicating an acceptable system loading resilience level, the rate of metric value under 0.85 (<=0.85) is 80% of the line outages cases which shows the

Authorized licensed use limited to: b-on: Universidade de Coimbra. Downloaded on April 27,2025 at 06:58:05 UTC from IEEE Xplore. Restrictions apply.

high probability of system with low resilience under the described initial operating conditions.

2) Generation Shedding and Power Incremental Apportion

Generation shedding usually occurs in a power system due to fault triggering or events that lead to major load drops external attacks. In this section, two scenarios are simulated. Scenario 1 is called "isolation," in which one generator (one of the generators at Buses 2, 3, 6, or 8) is disconnected, therefore the total generation power at this bus is lost. Scenario 2 is called "apportion," in which one generator is disconnected but the generation at other buses (except Bus 1) are increased to compensate for the generation power loss. The simulation results are shown in Table II.

TABLE II. THE METRIC VALUES DUE TO GENERATION SHEDDING

Bus No.	2	3	6	8
***r* of isolation**	0.9	1.0	0.85	0.8
***r* of apportion**	0.9	1.0	0.85	0.8

The values of the resilience metric (r) are 0.9, 1.0, 0.85 and 0.8 separately when a generator is disconnected at each PV bus in the two scenarios. The generation shedding in the IEEE 14-bus system leaves no serious impact on transmission lines compared to the threshold 0.85.

The simulation results show equal values of resilience metric (r) in each scenario, because there is no compensated power apportioning from other generators when one of the generators on Buses 3, 6 or 8 is isolated due to their 0 MW output.

For the disconnection of the generator at Bus 2, although the resilience metric (r) value stays the same for the "isolation" and "apportion" scenarios, the loading rates for individual transmission lines are different in the two scenarios. The resilience metric (r) provides an overall profile for the system, while the line loading rates provide detailed information for each transmission line. The loading rate of each transmission line in the two scenarios are shown in Fig. 6.

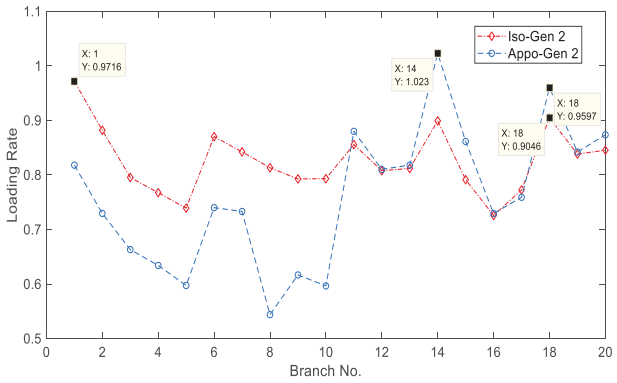

Fig. 6. The branch loading rate of generation shedding on Bus 2.

It should be noted that in the calculation for r, a transmission line is considered stressed if its loading is above 90% of its capacity. If the threshold for calculating r is changed from 90% to 80%, then the r for isolation scenario becomes 0.4 and for apportion scenario becomes 0.55.

The results of the isolation scenario are shown in red points and the results of the apportion scenario are shown in blue points. It can be seen that in the apportion scenario, overloading occurs on Branch 14, which is mainly because the real power of IEEE 14-bus system was mostly supported by slack bus in the base case.

3) Load Demand Increasing

The load demand at each load bus is increased by 10 MW at one time until the generation of slack bus reaches its maximum value. The metric values are shown in Fig. 7 with metric value in the cells. The load is numbered according to the order of loading bus.

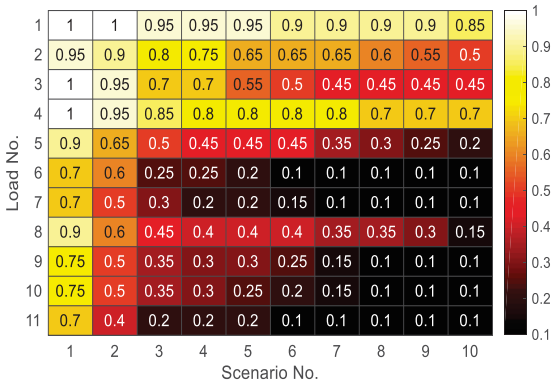

Fig. 7. The metric values in response to increasing the real power of each load by 10 MW from one scenario to the next.

From Fig. 7, it can be seen that increasing the load at Bus 11 is more serious than other loads. Load demand increase requires more transmission capacity, which matches the physical condition that the load located far from the source results in more severe overloading status of transmission lines.

The cases are performed using the IEEE 14-bus system to simulate the consequences of external attacks or large disturbances. The power flows in transmission lines are re-distributed according to the grid connections and generation/load locations. It is helpful to use an efficient way to display the status of transmission lines and capture the overall system state. The simulation results show that the status of transmission lines can be quantitated in various (e.g., generation shedding, load increasing, etc.) contingency conditions using the proposed resilience metric.

As shown in the generation shedding case, the metric value r stays the same for the isolation and apportion scenarios, because the r value is computed based on the percentage of the number of overloading branches without differentiating individual lines. This computation method captures the overall characteristics of the power grid. Further verification of the resilience metric is performed using the IEEE 118-bus system in Section IV.C.

C. Case Simulation using the IEEE 118-Bus System

There are 118 buses, 54 generators, 99 loads, and 186 transmission line and transformers in the IEEE 118-bus system [26]. The following are the results of contingency analysis

Authorized licensed use limited to: b-on: Universidade de Coimbra. Downloaded on April 27,2025 at 06:58:05 UTC from IEEE Xplore. Restrictions apply.

scenarios performed in comparison with the IEEE 14-bus system.

1) One Transmission Line Open

Simulation is performed by disconnecting the branches one by one. There are 186 scenarios in the open-line contingency analysis. The metric value (r) for each scenario is shown in Fig. 8.

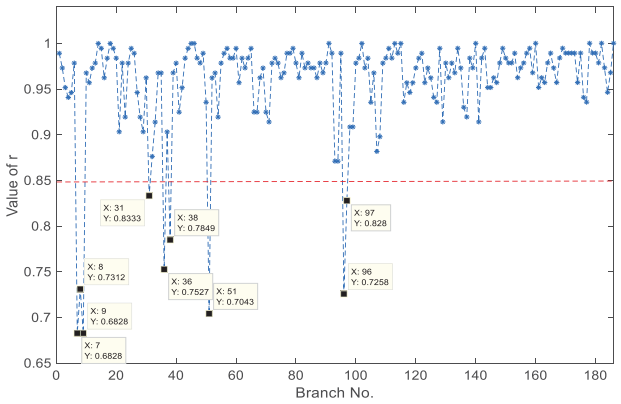

Fig. 8. The curve of metric value under open-line conditions.

From Fig. 8, it can be seen that there are 9 cases whose metric value is below 0.85. The rate is 4.84%. The values show that open-branch conditions due to permanent faults or potentially due to attacks impacting Branches 7 and 9 could cause more transmission lines to reach overloaded status. In contrast, opening some branches (e.g., branches 14, 18, and 45) has little effects on operation status.

2) Generation Shedding and Power Increment Apportion

One generator is isolated from system at a time, for contingency analysis, and the metric values are shown in Fig. 9.

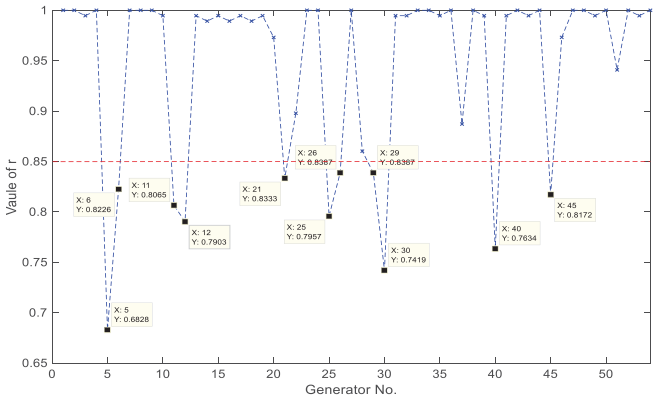

Fig. 9. The metric value of generation shedding.

As shown in Fig. 9, the metric values show that opening Generator No. 5 (at Bus 10) without increasing loading on other generators causes the largest number of transmission lines to fall below their margins and possibly some to be overloaded. In contrast, disconnecting some generators has no effects on branch overloading, since the r values remain at 1. The percentage of cases with metric values under 0.85 is 20.37% (11/54).

For the apportion of real power, the values of the proposed resilience metric are shown in Fig. 10. The slack bus is included in the figure, but the generator at the slack bus doesn't compensate for the power loss of the isolated generator. When the generator at the slack bus is isolated, the other generators can compensate for the lost generation in the system. The metric value in Fig. 10 shows that disconnecting the generator at the slack bus (Bus 30) does not cause any of the lines to fall below 10% capacity margins.

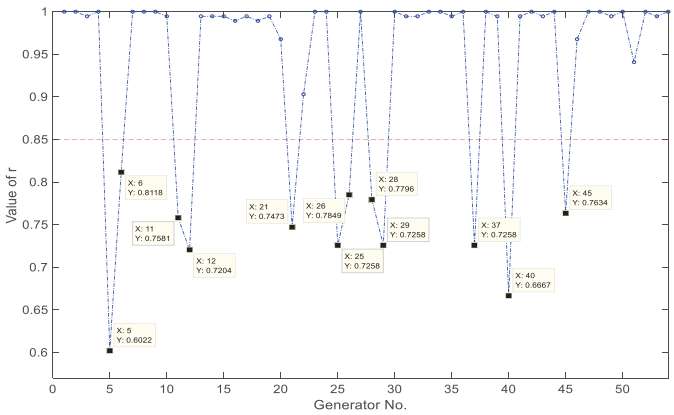

Fig. 10. The metric value of isolated generation apportioned by other generators.

From Fig. 10, the values below 0.85 show that the isolated generators still impact on the transmission lines, even with the other generators compensating for the load power supply. Similarly, the generator at Bus 5 is still the most critical to the system, and it causes most transmission lines to fall below 10% capacity margin or become overloaded.

The comparison of the two situations at the same generation bus shows different metric values, which reflects the change of transmission line operation status.

3) Load Demand Increasing

The load demand at each load bus is increased by 10 MW at one time until generation reaches its maximum value. The corresponding metric values are shown in Fig. 11.

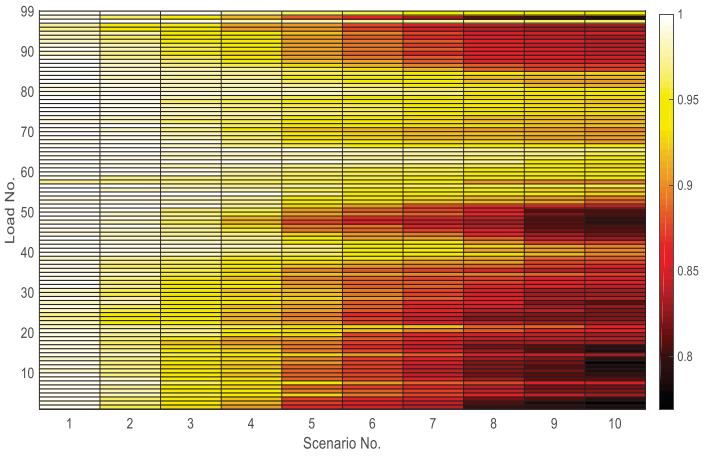

Fig. 11. The metric value of active load power increased by 10 MW at one time respectively.

Authorized licensed use limited to: b-on: Universidade de Coimbra. Downloaded on April 27,2025 at 06:58:05 UTC from IEEE Xplore. Restrictions apply.

From the results in Fig. 11, it can be seen that the number of branches falling below 10% capacity margin or becoming overloaded is large when the load demand is increased toward the limits of the slack bus. The changing trend is different with different branches, which shows that the load change brings different effects on branches. The simulation results are consistent with the situations in real power systems. Load increase brings about more impact to its adjacent branches.

V. Conclusion

In this paper, the relationship between system resilience and transmission line operation states is illustrated. A resilience metric is proposed based on the remaining power capacity of transmission lines, using the probability of loading rates to compute a system metric. The validity of the proposed resilience metric is verified with steady-state simulations in the IEEE 14-bus and 118-bus systems. The proposed resilience metric (r) clearly shows the capacity margin or overloading status of transmission lines, which provides quick information of the system overall operation margin for operators to use in addition to status of individual overloaded lines from the energy management system.

In our future work, the applicability of the proposed resilience metric to transient processes will be investigated. Also, resilience-based system operation strategies will be proposed using resilience metrics and optimization techniques so that operators can promptly make decisions on whether to further check details.

References

[1] J. Wang and H. Gharavi, "Power Grid Resilience," *Proceedings of the IEEE*, vol. 105, no. 7, pp. 1199-1201, 2017.

[2] J. Taft, "Electric grid resilience and reliability for grid architecture," Pacific Northwest National Laboratory. https://gridarchitecture. pnnl. gov/media/advanced/Electric_Grid_Resilience_and_Reliability. pdf (2017).

[3] Z. Bie, Y. Lin, G. Li, and F. Li, "Battling the extreme: A study on the power system resilience," *Proceedings of the IEEE*, vol. 105, no. 7, pp. 1253-1266, 2017.

[4] Y. Chakhchoukh, H. Lei, and B. K. Johnson, "Diagnosis of outliers and cyber attacks in dynamic PMU-based power state estimation," *IEEE Transactions on Power Systems*, vol. 35, no. 2, pp. 1188-1197, March 2020.

[5] K. Lingaraju, J. Gui, B. K. Johnson, and Y. Chakhchoukh, "Simulation of the Effect of False Data Injection Attacks on SCADA using PSCAD/EMTDC," in 52nd North American Power Symposium (NAPS), pp. 1-5, 2021.

[6] J. Lopez, J. E. Rubio, and C. Alcaraz, "A resilient architecture for the smart grid," *IEEE Transactions on Industrial Informatics*, vol. 14, no. 8, pp. 3745-3753, 2018.

[7] H. Lei, B. Chen, K. L. Butler-Purry, and C. Singh, "Security and reliability perspectives in cyber-physical smart grids," in 2018 IEEE Innovative Smart Grid Technologies-Asia (ISGT Asia), pp. 42-47, 2018.

[8] A. Ashok, M. Govindarasu, and J. Wang, "Cyber-physical attack-resilient wide-area monitoring, protection, and control for the power grid," *Proceedings of the IEEE*, vol. 105, no. 7, pp. 1389-1407, 2017.

[9] H. Lei and Chanan Singh, "Incorporating protection systems into composite power system reliability assessment," in 2015 IEEE Power & Energy Society General Meeting, pp. 1-5, 2015.

[10] M. Nazemi and P. Dehghanian, "Seismic-resilient bulk power grids: Hazard characterization, modeling, and mitigation," *IEEE Transactions on Engineering Management*, vol. 67, no. 3, pp. 614-630, 2019.

[11] K. Eshghi, B. K. Johnson, and C. G. Rieger, "Power system protection and resilient metrics," in IEEE 2015 Resilience Week (RWS), pp. 1-8, 2015.

[12] K. Eshghi, B. K. Johnson, and C. G. Rieger, "Metrics required for power system resilient operations and protection," in IEEE 2016 Resilience Week (RWS), pp. 200-203, 2016.

[13] T. Phillips, T. McJunkin, C. Rieger, J. Gardner, and H. Mehrpouyan, "An operational resilience metric for modern power distribution systems," in 2020 IEEE 20th International Conference on Software Quality, Reliability and Security Companion (QRS-C), pp. 334-342, 2020.

[14] T. R. McJunkin and C. G. Rieger, "Electricity distribution system resilient control system metrics," in IEEE 2017 Resilience Week (RWS), pp. 103-112, 2017.

[15] F. Liberati, A. D. Giorgio, A. Giuseppi, A. Pietrabissa, and F. D. Priscoli, "Efficient and Risk-Aware Control of Electricity Distribution Grids," *IEEE Systems Journal*, vol. 14, no. 3, pp. 3586-3597, 2020.

[16] F. Hafiz, B. Chen, C. Chen, A. R. de Queiroz, and I. Husain, "Utilising demand response for distribution service restoration to achieve grid resiliency against natural disasters," *IET Generation, Transmission & Distribution*, vol. 13, no. 14, pp. 2942-2950, 2019.

[17] C. Chen, J. Wang, F. Qiu, and D. Zhao, "Resilient distribution system by microgrids formation after natural disasters," *IEEE Transactions on Smart Grid*, vol. 7, no. 2, pp. 958-966, 2015.

[18] F. Z. Peng, "Flexible AC transmission systems (FACTS) and resilient AC distribution systems (RACDS) in smart grid," *Proceedings of the IEEE*, vol. 105, no. 11, pp. 2099-2115, 2017.

[19] T. Phillips, T. McJunkin, C. Rieger, J. Gardner, and H. Mehrpouyan, "A Framework for Evaluating the Resilience Contribution of Solar PV and Battery Storage on the Grid," in IEEE 2020 Resilience Week (RWS), pp. 133-139, 2020.

[20] T. Phillips, V. Chalishazar, T. McJunkin, M. Maharjan, S.M. S. Alam, T. Mosier, and A. Somani, "A metric framework for evaluating the resilience contribution of hydropower to the grid," in IEEE 2020 Resilience Week (RWS), pp. 78-85, 2020.

[21] B. Vaagensmith, T. McJunkin, K. Vedros, J. Reeves, J. Wayment, L. Boire, C. Rieger, and J. Case, "An Integrated Approach to Improving Power Grid Reliability: Merging of Probabilistic Risk Assessment with Resilience Metrics," in IEEE 2018 Resilience Week (RWS), pp. 139-146, 2018.

[22] G. Fu, S. Wilkinson, R. J. Dawson, H. J. Fowler, C. Kilsby, M. Panteli, and P. Mancarella, "Integrated approach to assess the resilience of future electricity infrastructure networks to climate hazards," *IEEE Systems Journal*, vol. 12, no. 4, pp. 3169-3180, 2017.

[23] R. D. Zimmerman, C. E. Murillo-Sanchez, and R. J. Thomas, "MATPOWER: Steady-state operations, planning, and analysis tools for power systems research and education," *IEEE Transactions on Power Systems*, vol. 26, no. 1, pp. 12-19, Feb. 2011.

[24] C. E. Murillo-Sanchez, R. D. Zimmerman, C. L. Anderson, and R. J. Thomas, "Secure planning and operations of systems with stochastic sources, energy storage and active demand," *IEEE Transactions on Smart Grid*, vol. 4, no. 4, pp. 2220-2229, Dec. 2013.

[25] B. Liu, F. Liu, B. Zhai, and H. Lan, "Investigating continuous power flow solutions of IEEE 14-bus system," *IEEJ Transactions on Electrical and Electronic Engineering*, vol. 14, no. 1, pp. 157-159, 2019.

[26] A. Raje, S. D. Varwandkar, and Anil Raje, "Deregulation analytics for security assessment in IEEE 118-bus system using modular power flow," in 2016 International Conference on Electrical Power and Energy Systems (ICEPES), pp. 321-326, 2016.

Authorized licensed use limited to: b-on: Universidade de Coimbra. Downloaded on April 27,2025 at 06:58:05 UTC from IEEE Xplore. Restrictions apply.